


Cite this: *Nanoscale Adv.*, 2019, 1, 305

# Flower-like 3-dimensional hierarchical $\text{Co}_3\text{O}_4/\text{NiO}$ microspheres for 4-nitrophenol reduction reaction

Amutha Chinnappan, <sup>\*a</sup> Saeideh Kholghi Eshkalak, <sup>ab</sup> Chinnappan Baskar, <sup>c</sup> Marziyeh Khatibzadeh, <sup>b</sup> Elaheh Kowsari<sup>d</sup> and Seeram Ramakrishna <sup>\*a</sup>

Aromatic nitro compounds are toxic and not biodegradable. Therefore, the elimination of nitro groups is very important. Metal catalysts play an important role in the catalytic transformation. We present here flower-like 3D hierarchical  $\text{Co}_3\text{O}_4/\text{NiO}$  microspheres, which are prepared by a chemical precipitation method. The as-prepared catalyst is characterized by FTIR, SEM, TEM, EDS, XRD, XPS and  $\text{N}_2$  sorption isotherms. They have shown different morphologies such as flower, nanocubes, and hexagonal structure at different calcined temperatures. The synthesized catalyst is tested and used for the reduction of 4-nitrophenol to 4-aminophenol in the presence of sodium borohydride as a reducing agent. The reaction takes place in an aqueous medium at room temperature. The bimetallic catalyst  $\text{Co}_3\text{O}_4/\text{NiO}$  showed good performance and reusability.

Received 11th June 2018  
Accepted 25th August 2018

DOI: 10.1039/c8na00029h

rsc.li/nanoscale-advances

## 1. Introduction

Aromatic nitro compounds are utilized in the production of drugs, pesticides, and industrial solvents. Nevertheless, these chemicals are not environmentally benign. Among them, 4-nitrophenol (4-NP) is considered as a pollutant by the US Environmental Protection Agency (EPA). It has high stability and solubility in water. Aromatic nitro compounds are highly toxic and not biodegradable. The elimination of nitro groups can be achieved by reduction to amines, which are less toxic and can undergo biodegradation easily. To dispose of this pollutant, many methods have been developed such as chemical oxidation, physical adsorption, physical absorption and microbial treatment. Chemical transformations of starting materials into desired final products usually require a number of chemical operations in which additional reagents, catalysts, solvents, *etc.* are used. Thus, in the course of the transformation, besides the desired products, many waste materials (chemical toxins) are produced. The waste should be regenerated, destroyed, or disposed of, but it consumes much energy and creates a heavy burden on the environment and causes ecological problems. It is of great importance to develop and use synthetic methodologies that minimize such problems. Therefore, one of the ways to achieve this target is to explore alternative expeditious

reaction conditions and eco-friendly reaction media to accomplish the desired chemical transformations with minimized by-products or waste as well as eliminating the use of conventional organic solvents wherever possible. Reduction is a fundamental transformation in organic synthesis and commercially is quite significant, as it can be used in the large scale preparation of pharmaceuticals and fine chemicals. A variety of reducing systems and methodologies are available to carry out reductions. All these methods have their own drawbacks which include the use of high-pressure reactors, high pressure/temperature or both, strong acid medium, hazardous molecular hydrogen, long reaction times, low yields, toxic solvents, and nonselective stoichiometric amounts of reagents. On the other side, 4-aminophenol (4-AP) is a strong intermediate in the synthesis of many drugs for example: paracetamol, phenacetin. Reduction of 4-nitrophenol to 4-aminophenol by sodium borohydride in an aqueous system is a well-known method. However, this reduction reaction would not take place without the presence of a metal catalyst.<sup>1–6</sup>

For many years, precious and non-precious transition metals have been used as efficient catalysts in catalytic reactions. Nevertheless, highly expensive metals such as platinum and palladium on carbon utilized for this kind of reaction are flammable when exposed to air and require an inert atmosphere. Moreover, it's expensive and difficult to separate these homogeneous catalysts from the reaction products and as a consequence, their commercial application is limited. Nanostructured transition metal oxides have had good performance in the catalytic reaction due to their extremely good physical and chemical properties compared to conventional and bulk materials.<sup>7–11</sup>

In recent years, many reports have been published on the 4-NP reduction reaction catalysts which include  $\text{AuCu@Pt}$

<sup>a</sup>Center for Nanofibers and Nanotechnology, Department of Mechanical Engineering, National University of Singapore, Singapore 119260. E-mail: mpecam@nus.edu.sg; seeram@nus.edu.sg

<sup>b</sup>Department of Polymer Engineering and Color Technology, Amirkabir University of Technology, Tehran, Iran

<sup>c</sup>THDC Institute of Hydropower Engineering and Technology Tehri, Uttarakhand Technical University, Dehradun, Uttarakhand, India 249001

<sup>d</sup>Department of Chemistry, Amirkabir University of Technology, Tehran, Iran



nanoalloys,<sup>3</sup> Au nanoparticles,<sup>12</sup> nickel(0) nanoparticles (Ni-NP) decorated on electrospun polymeric (polycaprolactone (PCL)/chitosan) nanofibers (Ni-NP/ENF),<sup>13</sup> Ag<sub>2</sub>S nanoparticles on reduced graphene oxide (Ag<sub>2</sub>S NPs/RGO) nanocomposites,<sup>14</sup> Fe<sub>2</sub>O<sub>3</sub>/3DOM BiVO<sub>4</sub>,<sup>15</sup> SiO<sub>2</sub>@Cu<sub>x</sub>O@TiO<sub>2</sub> heterostructures,<sup>16</sup> silver nanoparticles<sup>17</sup> and Ni nanoparticles.<sup>18–20</sup> Remarkably, with noble metal NPs, the catalytic reaction mostly occurs on the surface of the NPs but inside the NPs the majority of atoms are catalytically inactive. In order to avoid those problems, non-noble metals should be used. The presence of two different metal atoms can bring good catalytic activity and stability due to synergistic effects resulting from metal interactions.<sup>21,22</sup>

In our previous studies, we reported hypercross-linked porous polystyrene/IL networks with easy accessibility and excellent catalytic activity for the reduction of 4-nitrophenol to 4-aminophenol using NaBH<sub>4</sub> in an aqueous system at room temperature.<sup>23</sup> In continuation of our interest in exploring nanostructured catalysts for organic chemical transformations, we report here 3D hierarchical Co<sub>3</sub>O<sub>4</sub>/NiO microspheres as an efficient catalyst for the reduction of 4NP under environmentally friendly conditions. The bimetallic counterparts Co<sub>3</sub>O<sub>4</sub>/NiO reduced the requirement for high catalyst loading. They showed an excellent performance and make the catalyst reusable. To the best of our knowledge, this bimetallic 3D hierarchical Co<sub>3</sub>O<sub>4</sub>/NiO microspheres catalyst is the sole example for the reduction of 4NP to 4AP. The synthetic scheme is represented in Fig. 1.

## 2. Experimental section

### 2.1 Materials

All chemicals used were reagent-grade and used as received without further purification. CoCl<sub>2</sub>·6H<sub>2</sub>O, NiCl<sub>2</sub>·6H<sub>2</sub>O, urea, 4-nitrophenol and sodium borohydride were purchased from Sigma-Aldrich.

### 2.2 Characterization

Field Emission Scanning Electron Microscopy (FE-SEM, JEOL-6700F) and Field Emission Transmission Electron Microscopy

(FE-TEM, JEOL JEM-2010F) were used to analyze the morphology of Co<sub>3</sub>O<sub>4</sub>/NiO microspheres. The elemental analyses of nanostructures were determined by Field Emission Scanning Electron Microscope Energy Dispersive X-ray spectroscopy (FESEM-EDS) and X-ray photoelectron spectroscopy [(XPS), model: Kratos Axis Ultra<sup>DLD</sup>, it has done neutralization for insulating samples]. X-ray powder diffraction (XRD) was performed to know the crystal structure of the as-prepared catalysts. The surface area of the as-prepared catalysts was studied by nitrogen sorption isotherms on a NOVA 4200e Surface Area & Pore Size Analyzer.

### 2.3 Synthesis of 3D hierarchical Co<sub>3</sub>O<sub>4</sub>/NiO microspheres

The typical synthetic procedure for the 3D hierarchical Co<sub>3</sub>O<sub>4</sub>/NiO microspheres is as follows: an equivalent mixture of CoCl<sub>2</sub>·6H<sub>2</sub>O (0.021 mol), and NiCl<sub>2</sub>·6H<sub>2</sub>O (0.021 mol) is dissolved in water at room temperature. Urea (0.105 mol) was then added to the above solution and the reaction mixture was stirred vigorously with a magnetic stirrer at room temperature for 30 min. Then the reaction mixture was kept in the oil bath and the reaction temperature was raised to 100 °C for 10 h with constant stirring. After the completion of the reaction, the obtained precipitate was washed several times with distilled water. Then centrifuged at 5000 rpm for 10 min and dried at 80 °C overnight. The resulting powders [Co/Ni](OH)<sub>2</sub> were calcined at 400 °C, and 600 °C in the air for 2 h to obtain Co<sub>3</sub>O<sub>4</sub>/NiO microspheres.

### 2.4 Typical procedure for reduction of 4-nitrophenol

4-Nitrophenol (0.0014 mol) and Co<sub>3</sub>O<sub>4</sub>/NiO microspheres (30 mg) were taken in 10 mL of water in a round-bottomed flask. NaBH<sub>4</sub> (0.005 mol) was added to the above mixture slowly at room temperature with constant stirring. The progress of the reaction was monitored by TLC. After the completion of the reaction, the catalyst was separated by centrifuging and washed with distilled water and dried in a vacuum oven and subsequently reused for the next run. The product in the reaction mixture was extracted with ethyl acetate (4 × 20 mL). The

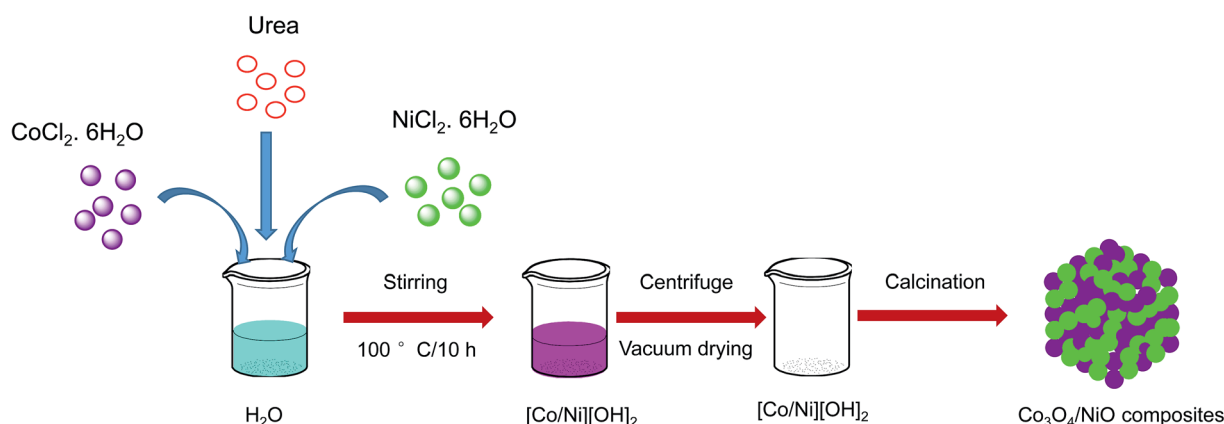


Fig. 1 Synthesis of flower-like 3D hierarchical Co<sub>3</sub>O<sub>4</sub>/NiO microspheres.





Fig. 2 SEM images: (a and b)  $[\text{Co/Ni}][\text{OH}]_2$ , (c and d)  $\text{Co}_3\text{O}_4/\text{NiO}$ -400 °C, (e and f)  $\text{Co}_3\text{O}_4/\text{NiO}$ -600 °C microsphere composites at low and high magnifications. Scale bars: 1  $\mu\text{m}$  in a, c, e; 100 nm in b, d, f.

organic layer was washed with brine, dried over  $\text{Na}_2\text{SO}_4$  and evaporated using reduced pressure.

### 3. Results and discussion

The synthesis of the 3D hierarchical  $\text{Co}_3\text{O}_4/\text{NiO}$  microspheres was studied with the optimized concentrations of the cobalt/nickel salts and urea in the aqueous system. The schematic representation is shown in Fig. 1. The completion of the reaction was indicated by the formation of precipitate. During the reaction, urea was hydrolyzed to release ammonia and  $\text{OH}^-$  ion, which further reacted with  $\text{Co}^{2+}/\text{Ni}^{2+}$  to form  $[\text{Co/Ni}][\text{OH}]_2$ . The obtained precipitate was washed several times with water, and dried in a vacuum oven at 80 °C overnight. The resulting powder was further calcined at different temperatures: 400 °C and 600 °C. The following reaction scheme illustrates the synthesis process of  $[\text{Co/Ni}][\text{OH}]_2$  and the  $\text{Co}_3\text{O}_4/\text{NiO}$  catalyst.

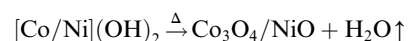
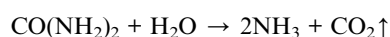


Fig. 2 shows the typical SEM images of (a and b)  $[\text{Co/Ni}][\text{OH}]_2$ , (c and d)  $\text{Co}_3\text{O}_4/\text{NiO}$ -400 °C, (e and f)  $\text{Co}_3\text{O}_4/\text{NiO}$ -600 °C microsphere composites at low and high magnifications. The overall  $\text{Co}_3\text{O}_4/\text{NiO}$  samples exhibited microsphere structures, which are composed of a number of ultra-thin nanoflakes. They are porous in nature and formed from several interconnected nanoparticles (such as nanocubes and hexagonal structures). The interconnected nanoflakes form flower-like structures within the microspheres changing to nanocubes and hexagonal structures by changing with annealing temperature. Fig. 2b shows the flower-like structure of the  $[\text{Co/Ni}][\text{OH}]_2$  catalyst and Fig. 2c–f exhibit  $\text{Co}_3\text{O}_4/\text{NiO}$  different morphologies at the different calcination temperatures of 400 °C and 600 °C. The mean particle size is also varied such as 55 nm for  $[\text{Co/Ni}][\text{OH}]_2$  and the calcined samples got 23 nm and 16 nm for  $\text{Co}_3\text{O}_4/\text{NiO}$ -400 °C and  $\text{Co}_3\text{O}_4/\text{NiO}$ -600 °C respectively. Fig. 3a and b show





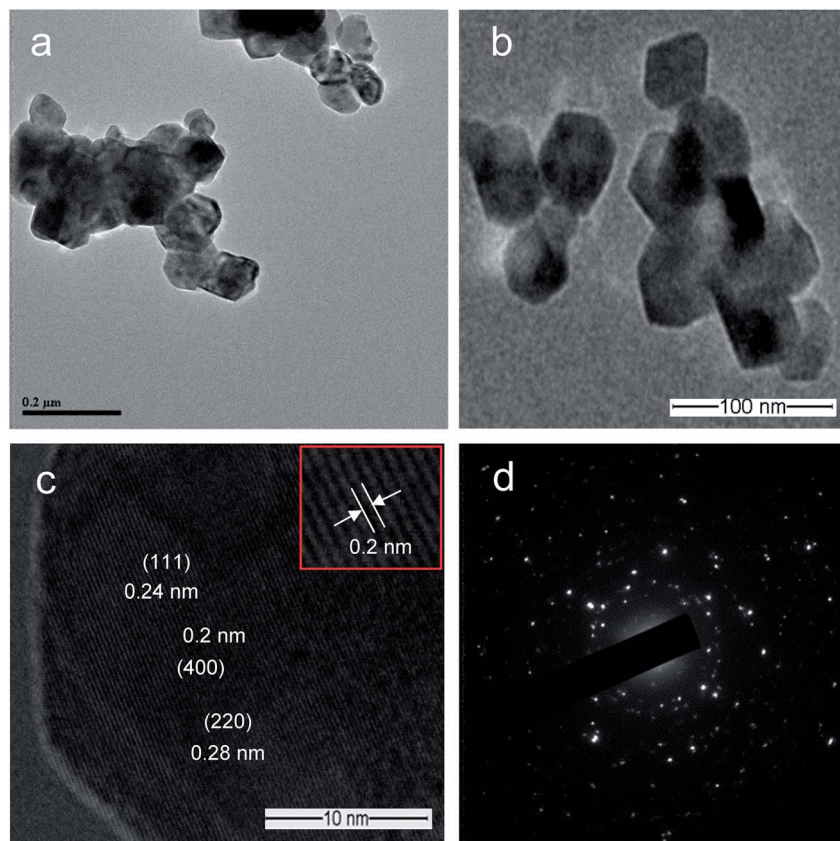


Fig. 3 TEM images of  $\text{Co}_3\text{O}_4/\text{NiO}$ -600 °C microspheres: (a and b) at high and low magnifications; (c) lattice plane; (d) SAED pattern.

the TEM image of  $\text{Co}_3\text{O}_4/\text{NiO}$  microspheres in high and low magnifications. TEM images showed that  $\text{Co}_3\text{O}_4/\text{NiO}$  microsphere have nanocubes and hexagonal structures. Fig. 3c shows the interplanar  $d$  spacings of 0.2 nm and 0.28 nm, which correspond to the crystal planes (400, 220) of  $\text{Co}_3\text{O}_4$  at interfacial angles of  $2\theta$  44.8° and 31.2°.  $\text{NiO}$  was also confirmed by the lattice spacing measurement (0.24 nm) at the interfacial angle of  $2\theta$  37.2°, which corresponds to the crystal plane of 111. The SAED pattern is shown in Fig. 3d. The scanning electron microscope and energy dispersive X-ray spectrometer (SEM-EDS) spectrum is given in Fig. 4a. The as-prepared, all  $\text{Co}_3\text{O}_4/\text{NiO}$  microspheres catalyst was analyzed by EDS and it showed the presence of Co, Ni and O. We present here the EDS spectra of  $\text{Co}_3\text{O}_4/\text{NiO}$ -600 °C. The elemental composition of Co (25.7%), Ni (16.1%) and O (58.1%) was predicted from the EDS analysis (atomic% is presented).

Fig. 4b illustrates the XRD patterns for different annealing temperatures of the 3D hierarchical  $\text{Co}_3\text{O}_4/\text{NiO}$  microspheres composite. All compounds showed a typical cubic crystal structure. Increasing heat treatment resulted in patterns with sharper diffraction lines. The characteristic peaks located at  $2\theta$  31.28°, 37.23°, 38.78°, 43.48°, 44.8°, 55.67°, 59.49°, 63.04°, 65.1°, 74.73°, 78.4° were ascribed to the  $\text{Co}_3\text{O}_4/\text{NiO}$  composites with cubic structure. The crystalline phases and the crystallite sizes of the powders were confirmed by XRD measurements. The reflection peaks of  $\text{Co}_3\text{O}_4/\text{NiO}$  microspheres, indexed to 111, 200, 220, 311, 222, 400, can be assigned to the cubic phase

of  $\text{Co}_3\text{O}_4/\text{NiO}$ .<sup>24,25</sup> The 3D microspheres were further characterized by X-ray photoelectron spectroscopy. The survey wide scan of the  $\text{Co}_3\text{O}_4/\text{NiO}$  microspheres is shown in Fig. 5a. The high-resolution XPS spectroscopy of Co 2p is shown in Fig. 5b; two important peaks at 791.9 eV and 776.9 eV are observed, corresponding to Co 2p<sub>1/2</sub> and Co 2p<sub>3/2</sub>, respectively. At the same time, two small satellite peaks are obtained at 786.8 and 801.8 eV. These could be attributed to  $\text{Co}^{3+}$ .<sup>25</sup> Similarly the 2p spectral region of Ni (Fig. 5c) shows two peaks at 867.3 eV and 850 eV corresponding to Ni 2p<sub>1/2</sub> and Ni 2p<sub>3/2</sub> respectively. These binding energies could be attributed to  $\text{Ni}^{2+}$ .<sup>24</sup> The O 1s spectrum (Fig. 5d) has two distinct components. The strong peak at 529.5 eV could be assigned to oxygen atoms in the oxides of  $\text{Co}_3\text{O}_4$  and  $\text{NiO}$ .<sup>24</sup> This is obtained after correcting the charging effect using the C 1s binding energy of adventitious carbon at about 284.6 eV.

The as-prepared catalysts were further analyzed by nitrogen sorption isotherms on a NOVA 4200e Surface Area & Pore Size Analyzer. Samples were degassed at 60 °C overnight under conditions of dynamic vacuum before analysis. The specific surface areas for  $\text{N}_2$  were calculated using the BET model over a relative pressure ( $P/P_0$ ). Total pore volumes were calculated from the uptake at a relative pressure of 0.990. The BET analysis was performed to scrutinize the textural properties of the as-prepared catalysts. Fig. 6a shows the  $\text{N}_2$  sorption isotherms of  $\text{Co}_3\text{O}_4/\text{NiO}$  catalysts at the different calcined temperatures of 400 °C and 600 °C. Fig. 6b depicts the sizes of the micro- and





Fig. 4 Co<sub>3</sub>O<sub>4</sub>/NiO-600 °C microspheres: (a) EDS mapping; (b) XRD.

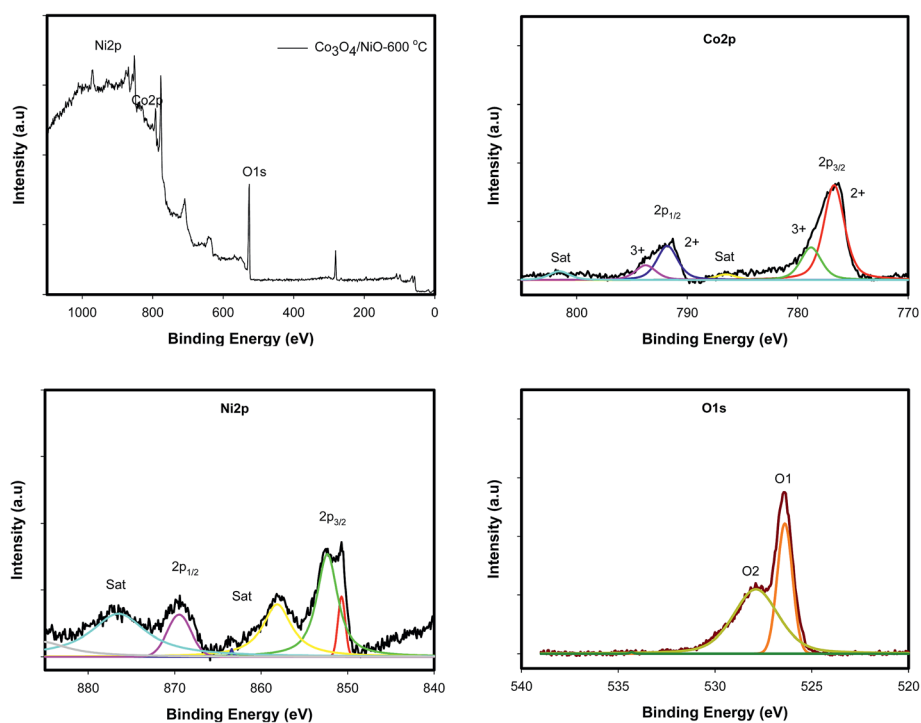


Fig. 5 XPS spectra of Co<sub>3</sub>O<sub>4</sub>/NiO-600 °C microspheres.





Fig. 6  $\text{Co}_3\text{O}_4/\text{NiO}$  microspheres: (a)  $\text{N}_2$  sorption isotherms; (b) micro- and mesopores distributions.

mesopores with an observed range of 1 nm to 55 nm. The  $\text{N}_2$  sorption isotherm of each catalyst exhibited a type IV or V, indicating the large mesopores. It may be due to the pores becoming filled with increased adsorbate. The BET surface area for  $\text{Co}_3\text{O}_4/\text{NiO-600 } ^\circ\text{C}$  was found to be  $6.244 \text{ m}^2 \text{ g}^{-1}$ , which was higher than the other calcined temperature  $\text{Co}_3\text{O}_4/\text{NiO-400 } ^\circ\text{C}$  ( $3.616 \text{ m}^2 \text{ g}^{-1}$ ). The corresponding pore volumes are  $0.03 \text{ cm}^3$ ,  $0.025 \text{ cm}^3$  respectively. The average pore diameters of the as-prepared 3D catalysts are 3.05 nm and 3.06 nm respectively. These materials have low surface areas and pore volumes. A similar decrease in surface area for mesoporous cobalt oxides was observed by Mogudi *et al.*,<sup>26</sup> and Song *et al.*<sup>27</sup>

Bimetallic nanoparticles are particularly useful due to the versatile composition and structural variations that may be

adjusted in order to improve catalytic behavior. Bimetallic catalysts frequently display catalytic activity that is higher than the constituent materials for reduction of 4-nitrophenol. Initially, the reduction of 4-nitrophenol to 4-aminophenol was carried out with as-prepared  $[\text{Co/Ni}][\text{OH}]_2$  and  $\text{Co}_3\text{O}_4/\text{NiO}$  microspheres catalyst in  $\text{NaBH}_4$  aqueous system at room temperature (Fig. 7). The reduction reaction completed in 60 min with  $[\text{Co/Ni}][\text{OH}]_2$  catalyst and gave 67% yield. The product yield is increased to 75% with  $\text{Co}_3\text{O}_4/\text{NiO-400 } ^\circ\text{C}$  and 80% with  $\text{Co}_3\text{O}_4/\text{NiO-600 } ^\circ\text{C}$  and the reaction time is reduced to 30 min and 20 min respectively. Therefore,  $\text{Co}_3\text{O}_4/\text{NiO-600 } ^\circ\text{C}$  is the best catalyst when compared to the other two catalysts,  $[\text{Co/Ni}][\text{OH}]_2$  and  $\text{Co}_3\text{O}_4/\text{NiO-400 } ^\circ\text{C}$ . The results are summarized in Table 1. To find out the importance of the above catalysts, we



Fig. 7 Possible mechanism of 4-nitrophenol reduction by 3D hierarchical  $\text{Co}_3\text{O}_4/\text{NiO}$  microspheres.



Table 1 Effect of different catalytic parameters on 4-nitrophenol reduction<sup>a</sup>

		Amount (mg)	Time (min)	Yield <sup>b</sup> (%)
Effect of different catalyst	[Co/Ni][OH] <sub>2</sub>	30	60	67
	Co <sub>3</sub> O <sub>4</sub> /NiO-400 °C	30	30	75
	Co <sub>3</sub> O <sub>4</sub> /NiO-600 °C	30	20	80
Effect of NaBH <sub>4</sub> on Co <sub>3</sub> O <sub>4</sub> /NiO-600 °C (molar ratio)	1 : 4	30	30	80
	1 : 8	30	30	86
	1 : 10	30	10	88
Effect of catalyst loading <sup>c</sup>	Co <sub>3</sub> O <sub>4</sub> /NiO-600 °C	20	30	77
		30	10	88
		50	10	88

<sup>a</sup> Reaction conditions: molar ratio: 1 : 8; 4-NP : NaBH<sub>4</sub>, H<sub>2</sub>O-10 mL, RT. <sup>b</sup> Isolated yield. <sup>c</sup> Molar ratio: 1 : 10; 4-NP : NaBH<sub>4</sub>.

have carried out the same reduction reaction under the same experimental conditions in the absence of the catalyst, it has been observed that no product was formed. It is well known that sodium borohydride is the source of hydrogen production for the reduction reaction but it needs the addition of a suitable amount of catalyst to progress the reduction reaction. To find out the effect of NaBH<sub>4</sub> on the as-prepared catalyst, we have chosen Co<sub>3</sub>O<sub>4</sub>/NiO-600 °C catalyst due to the best yield and economical reaction time. To optimize the minimum requirement of NaBH<sub>4</sub>, we have investigated the reduction reaction with different molar ratios (4-NP : NaBH<sub>4</sub>) such as 1 : 4; 1 : 8; and 1 : 10 with the catalytic amount of 30 mg Co<sub>3</sub>O<sub>4</sub>/NiO-600 °C at room temperature. It has been observed that 1 : 10 molar ratio was found to give the maximum yield (88%) of product with minimum reaction time (10 min). We have obtained 86% yield with 30 min reaction time for 1 : 8 molar ratio, and 80% yield for 1 : 4 molar ratio with 30 min reaction time. The results are summarized in Table 1. In order to find out the minimum requirement of catalyst Co<sub>3</sub>O<sub>4</sub>/NiO-600 °C for the reduction reaction, we have performed the reaction with different amounts which include 20 mg, 30 mg and 50 mg and the product yields were 77%, 88% and 88% respectively. The results are given in Table 1. Further increasing the amount of catalyst (50 mg) for the reduction transformation did not give any impact on the product yield and it remains the same as for 30 mg but we have observed that the reaction was completed within 10 min for 30 mg and 50 mg while 30 min was required for the reaction with 20 mg. The effect of catalytic performance gave a way to find out the mechanism of the catalyst. The possible mechanism of 4NP reduction with NaBH<sub>4</sub> in the aqueous system is shown in Fig. 7. It could catalyze this reaction by facilitating electron transfer from BH<sub>4</sub><sup>-</sup> to 4NP. Borohydride

ions are adsorbed onto the surface of the microspheres to react and transfer electrons to the Co<sub>3</sub>O<sub>4</sub>/NiO surface. The 4-NP anion reactant can be easily adsorbed onto the positively charged Co<sub>3</sub>O<sub>4</sub>/NiO catalyst. The existence of the excessive electrons added to the Co<sub>3</sub>O<sub>4</sub>/NiO microspheres facilitates the uptake of electrons by the adsorbed 4-NP molecule, which leads to the reduction of 4-NP to 4-AP. The cycle can start again with the product 4-AP leaving to make a free surface and this process repeating. A comparison of various catalysts used for the reduction of 4-nitrophenol is summarized in Table 2. It has been observed that all the other catalysts either took a longer reaction time to complete the reduction reaction or are highly expensive catalysts and all the reactions are carried out in organic solvents. Even though Pt/Pd catalysts showed a very good yield, the reaction time is longer and organic solvents are used in the reaction. Our reduction reaction conditions are very simple, convenient, fast, have a good yield and it is an environmentally benign methodology. The bimetallic Co<sub>3</sub>O<sub>4</sub>/NiO catalyst plays an important role in the reduction of 4-nitrophenol to 4-aminophenol.

The recovery and recyclability of the 3D Co<sub>3</sub>O<sub>4</sub>/NiO-600 °C microspheres catalyst has been studied in 4-NP with 10 mol of NaBH<sub>4</sub> in 10 mL distilled H<sub>2</sub>O and 30 mg of the as-prepared catalyst (Fig. 8b). The first run was carried out using freshly activated Co<sub>3</sub>O<sub>4</sub>/NiO-600 °C catalyst and >90% conversion and 88% yield was obtained. Upon completion of the reaction, the catalyst was filtered, washed with distilled H<sub>2</sub>O, and dried at 80 °C in a vacuum oven. Under these experimental conditions, similar results were obtained for the second cycle (86% yield). There was not much loss in the catalytic activity. However, in the third cycle, it was reduced a bit. This could be due to the recovery of the catalyst during work up. In order to confirm this,

Table 2 Comparison of various catalysts in 4-nitrophenol reduction

Catalyst	Reaction conditions	Time (min)	Yield (%)	Reference
Pt-Pd nanofibers	EtOAc/H <sub>2</sub> /RT	240	99	28
Ni nanoparticles	H <sub>2</sub> O/NaBH <sub>4</sub> /RT	2	98	29
Copper phthalocyanine complex	N <sub>2</sub> H <sub>4</sub> ·H <sub>2</sub> O ethylene glycol 70 °C	240	78	30
Nano copper	THF/H <sub>2</sub> O-50 °C	120	66	31
Nanocrystalline magnesium oxide-stabilized palladium (0)	THF/H <sub>2</sub> /RT	90	98	3
Cu <sub>67</sub> /Co <sub>17</sub> /Fe <sub>2</sub> O <sub>4</sub> /graphene	NaBH <sub>4</sub> /EtOH/H <sub>2</sub> O	12	99	32
3D Co <sub>3</sub> O <sub>4</sub> /NiO-600 °C microspheres (30 mg)	H <sub>2</sub> O/NaBH <sub>4</sub> /RT	10	88	This work





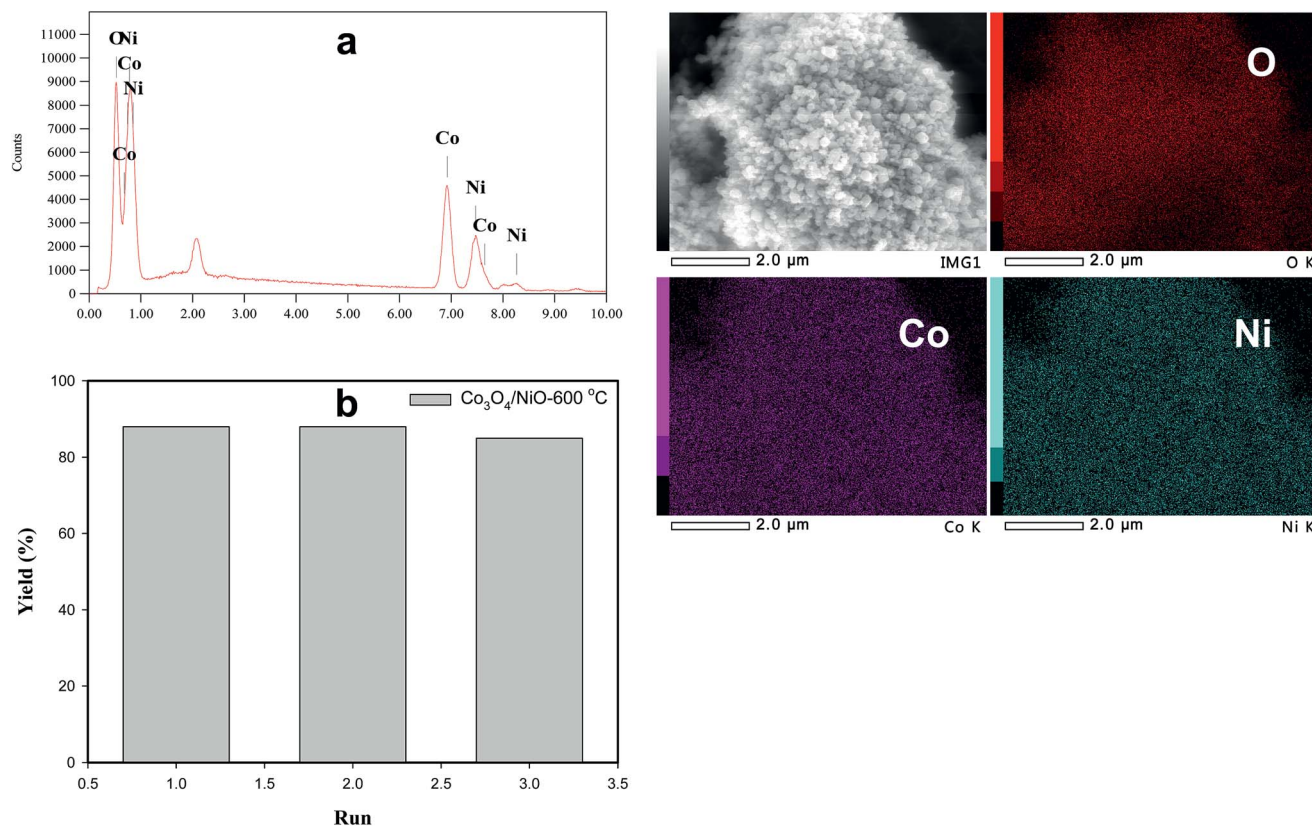


Fig. 8 (a) SEM-EDS spectrum of recycled catalyst; (b) number of run and % yield using recycled  $\text{Co}_3\text{O}_4/\text{NiO}$ -600 °C microspheres.

we have weighed the recycled catalyst; the amount was reduced from the initial weight 30 mg to 20 mg. The results of recycling experiments showed that the catalyst could be recycled at least 3 times without much loss in the catalytic activity. The recycled catalyst was analyzed using SEM and SEM-EDS as shown in Fig. 8a and it showed the same morphology as with the original one. It is very important to highlight here that the structure was not spoiled even after three cycles.

## 4. Conclusion

In conclusion, we have synthesized 3D hierarchical  $\text{Co}_3\text{O}_4/\text{NiO}$  microspheres and investigated the potential of  $[\text{Co/Ni}][\text{OH}]_2$ ,  $\text{Co}_3\text{O}_4/\text{NiO}$ -400 °C and  $\text{Co}_3\text{O}_4/\text{NiO}$ -600 °C for chemical transformation of 4-nitrophenol to 4-aminophenol. The 3D hierarchical  $\text{Co}_3\text{O}_4/\text{NiO}$  was prepared by a chemical co-precipitation method. The as-prepared catalyst showed different morphologies at different temperatures such as flower, nanocubes, and hexagonal structure and has been used for the reduction of 4-nitrophenol in the presence of  $\text{NaBH}_4$  with aqueous media at room temperature. The optimized reduction reaction is a simple, convenient procedure, with solvent-free conditions, easy work-up of the reaction mixture, good yield and an environmentally benign process to make this system as an attractive method and a synthetically useful addition to the present methodologies. Further efforts to extend the application of the catalyst  $\text{Co}_3\text{O}_4/\text{NiO}$  are underway in our laboratory.

## Conflicts of interest

There are no conflicts to declare.

## Acknowledgements

The authors thank the Lloyd's Register Foundation, UK (Project Number R265000553597 Nanotechnology in Sub-Sea Power Transmission) for research support and NUS Hybrid-Integrated Flexible (Stretchable) Electronic Systems Program (Grant Number R265000628133).

## Notes and references

- 1 L. Ai and J. Jiang, *Bioresour. Technol.*, 2013, **132**, 374–377.
- 2 S. Mehmood, N. K. Janjua, F. Saira and H. Fenniri, *J. Spectrosc.*, 2016, 6210794.
- 3 M. Lakshmi Kantam, R. Chakravarti, U. Pal, B. Sreedhar and S. Bhargava, *Adv. Synth. Catal.*, 2008, **350**, 822–827.
- 4 L. Liu, R. Chen, W. Liu, J. Wu and D. Gao, *J. Hazard. Mater.*, 2016, **320**, 96–104.
- 5 X. T. Shen, L. H. Zhu, G. X. Liu, H. W. Yu and H. Q. Tang, *Environ. Sci. Technol.*, 2008, **42**, 1687–1692.
- 6 J. Li, C. Y. Liu and Y. Liu, *J. Mater. Chem.*, 2012, **22**, 8426–8430.
- 7 M. Nemanashi and R. Meijboom, *Catal. Commun.*, 2016, **83**, 53–57.





- 8 Z. Jiang, J. Xie, D. Jiang, J. Jing and H. Qin, *CrystEngComm*, 2012, **14**, 4601–4611.
- 9 Y. Zhang, N. Zhang, Z. R. Tang and Y. J. Xu, *J. Phys. Chem. C*, 2014, **118**, 5299–5308.
- 10 B. Cornils and W. A. Herrman, *Applied Homogeneous Catalysis with Organometallic Compounds*, 2nd edn, Wiley-VCH, New York, 2002.
- 11 C. Burda, X. Chen, R. Narayanan and M. A. El-Sayed, *Chem. Rev.*, 2005, **105**, 1025–1102.
- 12 T. Ma, W. Yang, S. Liu, H. Zhang and F. Liang, *Catalysts*, 2017, **7**, 38.
- 13 K. Karakas, A. Celebioglu, M. Celebi, T. Uyar and M. Zahmakiran, *Appl. Catal., B*, 2017, **203**, 549–562.
- 14 B. Lang and H.-K. Yu, *Chin. Chem. Lett.*, 2017, **28**, 417–421.
- 15 K. Zhang, Y. Liu, J. Deng, S. Xie, H. Lin, X. Zhao, J. Yang, Z. Han and H. Dai, *Appl. Catal., B*, 2017, **202**, 569–579.
- 16 O. A. Zelekew and D.-H. Kuo, *Appl. Surf. Sci.*, 2017, **393**, 110–118.
- 17 C. Kästner and A. F. Thünemann, *Langmuir*, 2016, **32**, 7383–7391.
- 18 A. Wang, H. Yin, M. Ren, H. Lu, J. Xue and T. Jiang, *New J. Chem.*, 2010, **34**, 708–713.
- 19 A. Wang, H. Yin, H. Lu, J. Xue, M. Ren and T. Jiang, *Langmuir*, 2009, **25**, 12736–12741.
- 20 H. Lu, H. Yin, Y. Liu, T. Jiang and L. Yu, *Catal. Commun.*, 2008, **10**, 313–316.
- 21 Z. Dong, X. Le, C. Dong, W. Zhang, X. Li and J. Ma, *Appl. Catal., B*, 2015, **162**, 372–380.
- 22 O. Metin, S. F. Ho, C. Alp, H. Can, M. N. Mankin, M. S. Gultekin, M. Chi and S. Sun, *Nano Res.*, 2013, **6**, 10–18.
- 23 A. Chinnappan, A. H. Tamboli, W.-J. Chung and H. Kim, *Chem. Eng. J.*, 2016, **285**, 554–561.
- 24 C. Mahala and M. Basu, *ACS Omega*, 2017, **2**, 7559–7567.
- 25 H. Xia, D. Zhu, Z. Luo, Y. Yu, X. Shi, G. Yuan and J. Xie, *Sci. Rep.*, 2013, **3**, 2978.
- 26 B. M. Mogudi, P. Ncube and R. Meijboom, *Appl. Catal., B*, 2016, **198**, 74–82.
- 27 W. Song, A. S. Poyraz, Y. Meng, Z. Ren, S.-Y. Chen and S. L. Suib, *Chem. Mater.*, 2014, **26**, 4629–4639.
- 28 M. Takasaki, Y. Motoyama, K. Higashi, S.-H. Yoon, I. Mochida and H. Nagashima, *Org. Lett.*, 2008, **10**, 1601–1604.
- 29 R. J. Kalbasi, A. A. Nourbakhsh and F. Babaknezhad, *Catal. Commun.*, 2011, **12**, 955–960.
- 30 U. Sharma, P. Kumar, N. Kumar, V. Kumar and B. Singh, *Adv. Synth. Catal.*, 2010, **352**, 1834–1840.
- 31 Z. Duan, G. Ma and W. Zhang, *Bull. Korean Chem. Soc.*, 2012, **33**, 4003–4006.
- 32 H. Zhang, Y. Zhao, W. Liu, S. Gao, N. Shang, C. Wang and Z. Wang, *Catal. Commun.*, 2015, **59**, 161–165.

